

Research article

Efficient single-step reactive compatibilization of hemp flour-reinforced PLA/TPS blends: Exploring eco-friendly alternatives and bio-based compatibilizers from maleinized hemp oil

Alejandro Lerma-Canto¹, Ivan Dominguez-Candela², Jaume Gomez-Caturla¹,
Vicent Fombuena^{1*}, Daniel Garcia-Garcia¹

¹Instituto de Tecnología de Materiales (ITM), Universitat Politècnica de València (UPV), Plaza Ferrándiz y Carbonell 1, 03801 Alcoy, Spain

²Instituto de Seguridad Industrial, Radiofísica y Medioambiental (ISIRYM), Universitat Politècnica de València (UPV), Plaza Ferrándiz y Carbonell, s/n 03801 Alcoy, Spain

Received 11 October 2023; accepted in revised form 8 November 2023

Abstract. In a blend of poly(lactic acid) (PLA) and thermoplastic starch (TPS), a 15% load of hemp seed lignocellulosic filler (HF) was incorporated. Additionally, separate petrochemical-based compatibilizers, such as dicumyl peroxide (DCM) and benzoyl peroxide (LRL), as well as a bio-based compatibilizer, maleinized hemp seed oil (MHO), were introduced. Adding HF to the PLA/TPS blend reduced tensile mechanical properties due to the stress concentration phenomenon arising from the lack of interaction between components, yielding a more brittle material. This issue was mitigated by adding compatibilizers, notably the incorporation of MHO into the PLA/TPS/HF blend this increased elongation at break by enhancing compatibility among the blend components and providing a plasticizing effect. Moreover, regarding thermal properties, it was observed that the inclusion of HF led to a decrease in the glass transition temperature (T_g), cold crystallization temperature (T_{cc}), and melting temperature (T_m). Conversely, adding MHO to this blend increased all these values compared to the PLA/TPS/HF mixture, attributed to the plasticizing effect imparted by the modified oil. Additionally, following fracture in Charpy impact testing, the samples were subjected to field emission scanning electron microscopy (FESEM) analysis to examine the fractured surface of the various samples.

Keywords: maleinized hemp seed oil, hemp seed flour, poly(lactic acid) (PLA), thermoplastic starch (TPS), compatibilizers

1. Introduction

Poly(lactic acid) (PLA) is one of the most extensively studied biopolymers. It possesses a series of properties such as excellent mechanical properties [1], high transparency resulting from its high crystallinity [2], and great ease of processing through highly productive techniques like extrusion and injection molding [3]. Besides its technical features, PLA boasts competitive pricing, the capability of derivation from biomass, and biodegradability [4]. These

attributes place it favorably against other biopolymers, making it an ideal choice for applications in sectors like packaging and wrapping [5]. However, in order to be applied effectively at an industrial level, it is necessary to improve certain properties of PLA. The main drawbacks include its limited elongation capacity, low flexibility, and low toughness, making it excessively rigid for certain applications [6]. Melt blending PLA with other more ductile polymers is an efficient and cost-effective technique to

*Corresponding author, e-mail: vifombor@upv.es

© BME-PT

enhance its ductile properties [7]. Multiple studies have demonstrated the effectiveness of blending PLA with non-renewable ductile polymers, such as low-density polyethylene (LDPE). Wang *et al.* [8] showed that crystallinity is a key parameter in the toughness of PLA/LDPE blends. Reddy and Hillmyer [9] conducted blends of PLA with polypropylene (PP), increasing ductile properties and hydrolysis resistance but, of course, reducing biodegradability. Other studies have been conducted along the same lines with the use of polyamide (PA) [10] or polystyrene (PS), demonstrating a thermal stabilization of the blend despite the confirmed two glass transition temperatures (T_g), which indicated the immiscibility of the polymers [11].

To avoid compromising the biodegradability and compostability of PLA, multiple studies have explored blends of PLA with other biodegradable polymers. As examples of these studies, Iannace *et al.* [12] and Takagi *et al.* [13] conducted blends of PLA with polyhydroxyalkanoates (PHA). The studies demonstrated that the toughness of the blends was slightly increased due to weak interactions, but the lack of miscibility between the polymers led to compatibility issues. A similar effect has been observed in blends formed by PLA and poly(caprolactone) PCL [14], poly(butylene succinate) (PBS) [15], or thermoplastic starch (TPS) [16]. Blends of PLA and TPS (or starch) offer several advantages, such as low density, low cost, and improved thermal resistance. However, the lack of miscibility results in poor interfacial adhesion. Furthermore, the potential moisture absorption by TPS granules can lead to reduced moisture resistance and accelerated aging [17]. Furthermore, when adding natural fillers to these blends, which can reinforce mechanical properties, and barrier properties, improve biodegradability and reduce costs, proper phase compatibility becomes crucial [18].

One of the primary methods for enhancing phase compatibility is reactive compatibilization. During this process, a dispersed domain is formed in a low proportion, which facilitates physical and chemical interaction between phases [19]. This chemical reaction, occurring between two polymers or even between a polymer and a filler, enhances interfacial adhesion, resulting in a better balance of properties. Numerous studies have conducted reactive compatibilization processes between PLA and TPS. Some of the most commonly used compatibilizers include maleic anhydride (MA) [20], silane coupling agents

[21], citric acid (CA) [22], isocyanate-based compounds [23], and even itaconic acid (IA) [24].

Of the different reactive compatibilizers, maleic anhydride (MA) can be taken as a reference due to its good balance of properties, including low self-reactivity in the presence of free radicals and low toxicity and cost [25]. Various studies have shown how MA can react with the hydroxyl groups present in PLA and TPS. However, the efficiency of the reaction has been demonstrated to improve when a peroxide initiator is also used. One of the most commonly used initiators is 2,5-bis(tert-butylperoxy)-2,5-dimethyl hexane, commonly known as Luperox, from a petrochemical source [26]. In these types of studies, the combination of peroxide and MA significantly increases the phase interaction, enhancing the strength of blends based on PLA/TPS. Other studies demonstrate the efficiency of treatment with alternative peroxides such as dicumyl peroxide (DCM) [20] or even a potentially bio-based peroxide like lauroyl peroxide (LRL) [27]. These studies often involve prior functionalization of PLA, transforming it into PLA-g-MA, and subsequently carrying out the extrusion process, resulting in a two-step transformation of the blend [28]. Research on functionalization using reactive compatibilizing agents in a single step is less common.

Hence, the current study aims, firstly, to evaluate the efficiency of reactive compatibilization in a single step using a combination of reference reagents, consisting of MA and DCM, and MA and LRL (possibly obtainable from bio-based sources). Secondly, it seeks an ecological alternative to these reagents, which is where the use of bio-based plasticizers comes into play. The use of triglycerides can be an alternative to increase the fragility of PLA, but they will not react with the hydroxyl groups of PLA or even TPS by themselves because both PLA and TPS are hydrophilic, while triglycerides are hydrophobic [29]. This can lead to phase separation. This issue can be resolved by chemically modifying the oils through processes such as epoxidation or maleinization. In these modifications, epoxy or maleic groups are anchored to the triglycerides, enabling them to interact with the hydroxyl groups. Furthermore, the high molecular weight of these triglycerides minimizes the known problem of possible plasticizer migration, which can cause stiffening and aging of the blend. The limited bibliography found up to this point evaluates the use of maleinized linseed oil

(MLO) in PLA/TPS blends [30], but despite that, demonstrated the efficiency of maleinized hemp oil (MHO) for the compatibilization/plasticization of PLA [31], no studies have been found in PLA/TPS blends.

In the present study, composites consisting of PLA and TPS as biopolymer matrices are developed, with the addition of 15% by weight of hemp flour (HF) as a natural filler. This HF is obtained as a byproduct of the hemp oil extraction process and is chemically modified into MHO. The reuse of this lignocellulosic residue from hemp seeds avoids the potential drawbacks associated with the use of natural fibers, such as increased pressure on natural resources, forest preservation, biodiversity, and the acquisition of low-cost raw materials. The composites are developed with three types of reactive compatibilizers, namely DCM, LRL, and MHO. The first two are widely used in scientific research as reactive compatibilizers, but the use of MHO as a reactive compatibilizer and plasticizer is still relatively unexplored. The study conducts a comparative analysis of the main mechanical, thermal, colorimetric, and biodegradative properties of the developed composites, aiming to assess whether MHO is a technically, ecologically, and economically viable alternative to the current commercially employed reactive compatibilizers.

2. Experimental

2.1. Materials

Poly(lactic acid) (PLA) with a commercial-grade 3251D was supplied by NatureWorks LLC (Minnetonka, MN, USA). Its melt flow rate was $80 \text{ g} \cdot 10 \text{ min}^{-1}$ at $210 \text{ }^\circ\text{C}$ and its density was $1.24 \text{ g} \cdot \text{cm}^{-3}$. Thermoplastic starch (TPS) with a commercial-grade Mater-Bi[®]NF 866 was supplied by Novamont SPA (Novara, Italy). TPS was characterized by a melt flow rate of $3 \text{ g} \cdot 10 \text{ min}^{-1}$ at $150 \text{ }^\circ\text{C}$ with a load of 5 kg and a melting temperature of 110 to $120 \text{ }^\circ\text{C}$. In addition, dicumyl peroxide (DCM), maleic anhydride (MA), and Luperox[®] A75 Benzoyl peroxide (LRL) were supplied by Sigma Aldrich (Madrid, Spain). On the other hand, a residual cake obtained after cold pressing extraction of hemp seed oil (HSO), using a CRZ-309 press machine (Changyouxin Trading Co., Zhucheng, China), from whole hemp seed supplied by a local market (Callosa de Segura, Spain) was used as a lignocellulosic filler.

The residual cake was ground using a centrifugal mill from Retsch GmbH (Düsseldorf, Germany) at 8000 rpm and equipped with a 0.25 mm sieve. The hemp flour (HF) obtained after milling was used as the lignocellulosic filler. Finally, HSO was modified to obtain maleinized hemp seed oil (MHO) following the method used in previous studies [31]. The chemical structure of each compatibilizer is shown in Figure 1.

First of all, PLA and TPS pellets were dried at $50 \text{ }^\circ\text{C}$ for 24 h to remove dampness. Similarly, the HF was dried at $50 \text{ }^\circ\text{C}$ for 24 h before processing. A fixed weight content of PLA and TPS of 80 and 20 wt%, respectively. As for the amount of HF, it was set at 15%.

2.2. Sample processing

Before preparing the composites, PLA, TPS, and HF were dried at $45 \text{ }^\circ\text{C}$ in an air oven to remove the residual moisture. All samples were reweighed according to the proportions given in Table 1 and following the process outlined in previous related literature. All samples were processed in a Dupra S.L. (Castalla, Alicante, Spain) corotating extruder at a constant rate of 40 rpm. The temperature profile for extrusion from the hopper to the output was set as follows: 163, 165, 170, and $175 \text{ }^\circ\text{C}$. After extrusion, the samples obtained were cooled at room temperature and pelletized. Before injection, all extruded samples were allowed to dry again at $50 \text{ }^\circ\text{C}$ for 24 h. Once the mixtures were dried, they were made into pieces by injection molding in a Mateu & Solé machine (Barcelona, Spain). The temperature profile was set as follows: 190, 195, 197, and $200 \text{ }^\circ\text{C}$, from the hopper to the injection nozzle. The filling time was set to 1 s and the cooling time to 10 s.

2.3. Characterization techniques

2.3.1. Mechanical properties

Mechanical tests were performed to evaluate the influence of compatibilization effects on PLA/TPS/HF composites. These tests included tensile characterization, impact strength measurement, and hardness determination. Tensile characterization was performed using an Ibertest ELIB 30 universal testing machine from SAE Ibertest (Madrid, Spain). Specimens with dimensions of $150 \times 10 \times 4 \text{ mm}$ were used, following the recommendations of ISO 527. A load cell of 5 kN and a crosshead speed of $10 \text{ mm} \cdot \text{min}^{-1}$

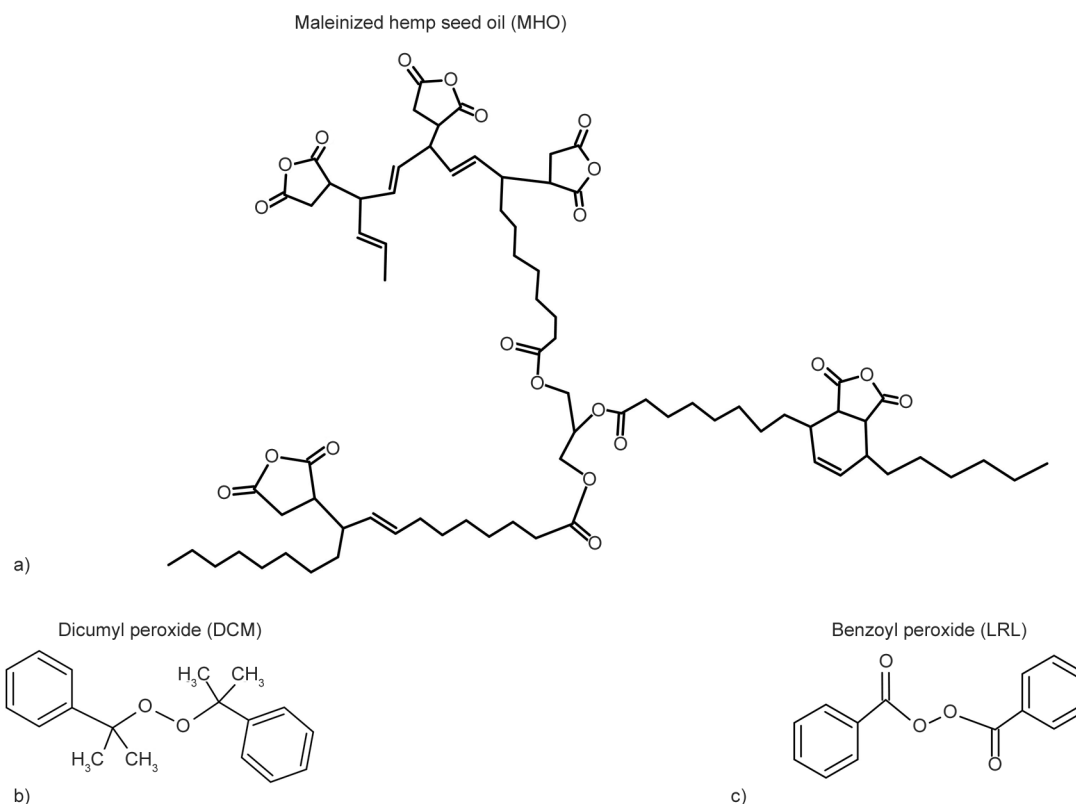


Figure 1. Scheme of the chemical structure of different compatibilizers used. a) Maleinized hemp seed oil (MHO), b) dicumyl peroxide (DCM), c) benzoyl peroxide (LRL).

Table 1. Composition of compatibilized and non-compatibilized PLA/TPS/HF samples.

Sample	PLA [wt%]	TPS [wt%]	HF [%]	MA [phr]	DCM [phr]	MHO [phr]	LRL [%]
PLA/TPS	80	20	–	–	–	–	–
PLA/TPS/HF	80	20	15	–	–	–	–
DCM	80	20	15	2	0.1	–	–
MHO	80	20	15	–	–	7.5	–
LRL	80	20	15	2	–	–	1

were applied. In addition, an SAE Ibertest axial extensometer was used to obtain the tensile modulus accurately.

The impact strength was measured with a 1 J Charpy pendulum manufactured by Metrotec SA (Madrid, Spain). The specimens had dimensions of 80×10×4 mm, according to the guidelines specified by ISO 179. In addition, hardness was assessed using a J. Bot SA (Barcelona, Spain) model 676-D Shore D durometer, as suggested by ISO 868.

All mechanical tests were performed at room temperature, and a minimum of five specimens per sample were tested to obtain the corresponding mean values and standard deviations. The analysis of these mechanical results will allow a better understanding of the properties and behavior of PLA/TPS/HF composites, as well as evaluate the effectiveness of

compatibilization effects in improving the mechanical properties of these composites.

2.3.2. Field emission scanning electron microscopy (FESEM)

Fractured surface morphologies resulting from impact testing of PLA/TPS/HF composites incorporating various compatibilizers were examined using field emission scanning electron microscopy (FESEM). FESEM measurements were performed using a ZEISS ULTRA 55 microscope, provided by Oxford Instruments (Oxfordshire, UK), with an operating accelerating voltage of 2 kV. Before the examination, a thin layer of Au-Pd alloy was applied to all fractured surfaces using a Leica Microsystems EM MED020 sputter coater (Wetzlar, Germany) under vacuum conditions for 120 s.

2.3.3. Differential scanning calorimetry (DSC)

The thermal behavior of PLA/TPS/HF composites incorporating various compatibilizers was investigated by differential scanning calorimetry (DSC). The primary thermal transitions of the PLA/TPS/HF composites were determined by DSC measurements using a Mettler-Toledo 821e calorimeter from Mettler Toledo Inc (Schwerzenbach, Switzerland). A dynamic temperature program was applied, consisting of an initial heating from 30 to 300 °C to eliminate any thermal history, followed by a cooling cycle from 300 to 30 °C, and finally, a heating program from 30 to 300 °C. Each sample, with an average weight of approximately 5–10 mg, was subjected to a cooling and heating rate of 10 °C·min⁻¹ according to ASTM D3418. All thermal cycles were performed under a nitrogen atmosphere, maintaining a constant flow rate of 66 ml·min⁻¹. The degree of crystallinity (X_c) of the compounds was determined by the Equation (1):

$$X_c [\%] = \frac{\Delta H_m - \Delta H_{cc}}{w \cdot \Delta H_m^0} \cdot 100 \quad (1)$$

where w denotes the weight fraction attributed to PLA. ΔH_m represents the enthalpy of fusion [J·g⁻¹], ΔH_{cc} stands for the enthalpy of cold crystallization [J·g⁻¹], and ΔH_m^0 denotes the enthalpy of fusion for a theoretically fully crystalline PLA structure, which according to the literature, is 93 J·g⁻¹ [32].

2.3.4. Thermogravimetric analysis (TGA)

The thermal stability of the composites was evaluated by TGA analysis performed on a TGA/SDTA 851 thermobalance manufactured by Mettler-Toledo Inc (Schwerzenbach, Switzerland). Each sample, with an average weight of approximately 10 mg, was subjected to a dynamic heating ramp from 30 to 700 °C at a constant heating rate of 10 °C·min⁻¹. All experiments were performed under a continuous nitrogen gas flow at a 66 ml·min⁻¹ rate. In addition, the onset temperature of degradation (T_0) was determined as the temperature at which a 5% weight loss was observed in the sample. The temperature at which the maximum degradation rate (T_{max}) was identified from the peak of the first derivative curve (DTG).

2.3.5. Melt flow index

An extrusion plastometer with a melt flow indexer and cutting mechanism, manufactured by Metrotec (Lezo, Spain), was used to determine the melt flow

index (MFI). The loading mass was set at 2.16 kg, and the temperature was kept at 190 °C. Each sample, weighing approximately 20 g, was placed in the indexer, and after a heating period of 2 min, the load was applied, initiating the flow of the material. Intervals of 30 s were set, during which samples of each material were collected and their masses were measured when the shear mechanism was activated. A total of five tests were performed for each mixture.

2.3.6. Disintegration under compost conditions

In accordance with ISO 20200, the evaluation of disintegration was carried out under aerobic conditions at 58 °C with a relative humidity of 55%. Rectangular samples of 25×25×1 mm were tightly enclosed in a containment bag and immersed in a controlled soil environment. The samples were subjected to a 24 h drying process at 40 °C to remove any remaining moisture before being weighed. The soil composition used for burial comprised sucrose, specialized rabbit feed, urea, maize starch, sawdust, maize oil, and mature compost, according to the proportions prescribed in ISO 20200. Over 35 days, the disintegration process was carried out, which involved periodic digging up of the samples on days 7, 9, 14, 17, 21, 28, and 35. After recovery, the samples were carefully rinsed with distilled water, subjected to 24 h exposure in an air oven at 40 °C, and reweighed. To ensure robustness, all experiments were performed in triplicate. The percentage of weight loss (W_L) was determined by Equation (2):

$$W_L [\%] = \frac{w_0 - w}{w_0} \cdot 100 \quad (2)$$

where w_0 represents the initial weight of the sample after the drying process, while w corresponds to the weight of the sample collected from the composted soil at various time points after drying. In addition, optical images were captured to document the time evolution of the disintegration process.

3. Results and discussion

3.1. Mechanical properties of PLA/TPS samples

The tensile mechanical properties of the different PLA/TPS samples can be seen in Figure 2. The PLA/TPS blend shows a tensile strength (Figure 2b) of 46.8 MPa, Young's modulus (Figure 2a) of 2300 MPa, and an elongation at a break (Figure 2c) of 6.7%. These values are similar to those obtained

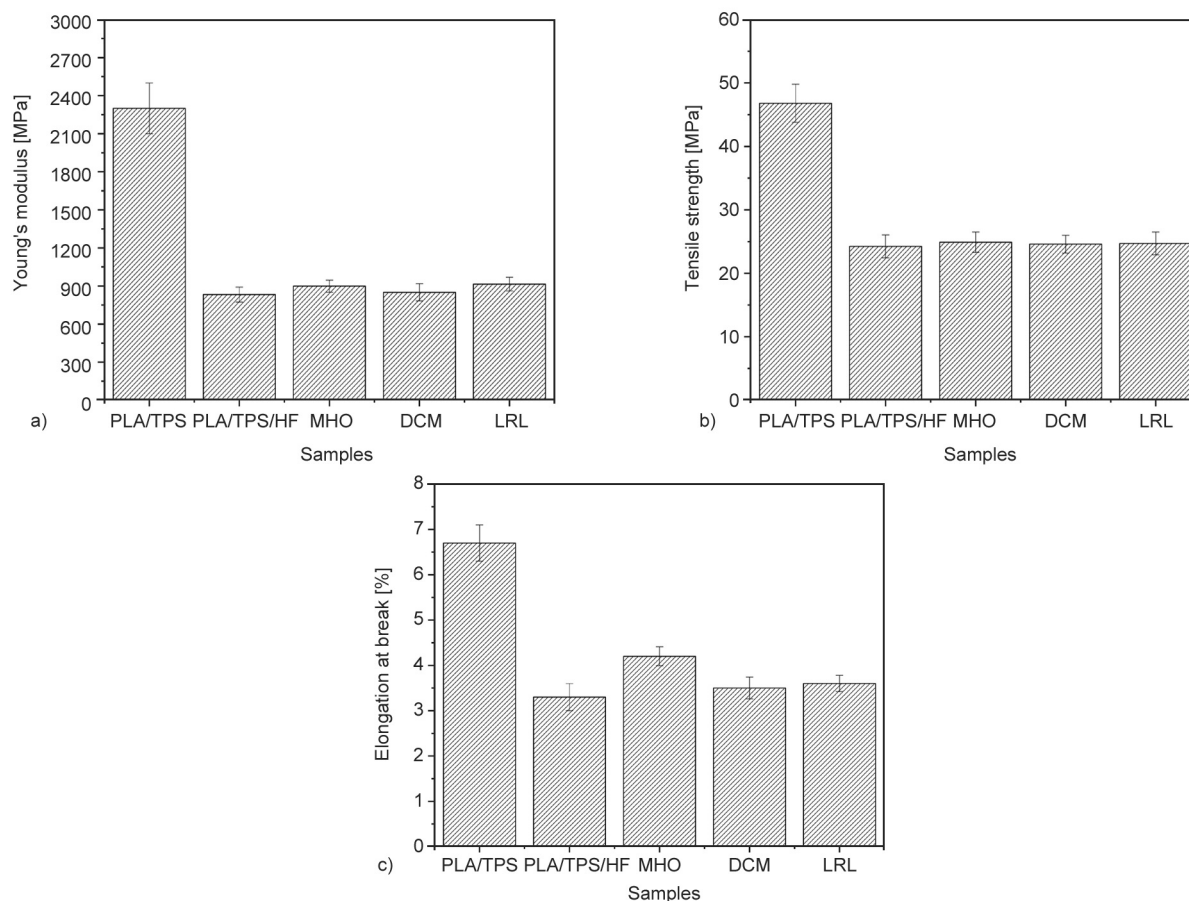


Figure 2. Tensile mechanical properties of PLA/TPS sample and PLA/TPS/HF samples without compatibilizer and compatibilized: a) Young's modulus, b) tensile strength, and c) elongation at break.

by Ghari and Nazockdast [33] for PLA/TPS samples. The incorporation of HF in the blend results in a significant reduction of the tensile mechanical properties. This is typical for composites reinforced with natural fibers, as their incorporation leads to stress concentration phenomena due to the lack of interaction between the HF residue and the matrix, resulting in the brittleness of the material [34]. In this case, the PLA/TPS sample reinforced with HF presents compatibilizers Young's modulus of 833 MPa, a tensile strength of 24.3 MPa, and an elongation at break of 3.3. On the other hand, it can be observed how the incorporation of the different compatibilizers hardly affects the tensile properties of the non-compatibilized sample (PLA/TPS/HF), obtaining very similar values of Young's modulus, tensile strength, and elongation at break. However, a slight increase in the elongation at the break of the reinforced blend can be observed after the incorporation of MHO, from 3.3 to 4.2% for the compatibilized sample, representing an increase of 27.3%. This increase in the elongation at break is due to the improved compatibility between PLA and TPS and

PLA/TPS and HF caused by MHO, as well as the plasticizing effect of MHO [35, 36].

On the other hand, Figure 3 shows the Shore D hardness and impact absorption energy of the PLA/TPS sample and of the PLA/TPS/HF composites without compatibilization and compatibilized PLA/TPS/HF composites. As can be seen in Figure 3, the incorporation of HF in the PLA/TPS blend resulted in a remarkable reduction of the impact absorption energy from $29.3 \text{ kJ}\cdot\text{m}^{-2}$ for the unreinforced blend to $9.9 \text{ kJ}\cdot\text{m}^{-2}$ for the blend reinforced with 15 wt% HF, a decrease of about 66.2%. This decrease in impact absorption energy is due to the lack of continuity of the matrix due to the low interaction between the polymeric matrix and the lignocellulosic residue, generating stress concentration points in the region of the particle-polymer interface, which facilitate the formation of micro-cracks and their propagation when the material is subjected to impact, embrittling the material. Incorporating the compatibilizers into the reinforced PLA/TPS sample slightly increases the impact absorption energy. This increase is more noticeable in the sample compatibilized with MHO,

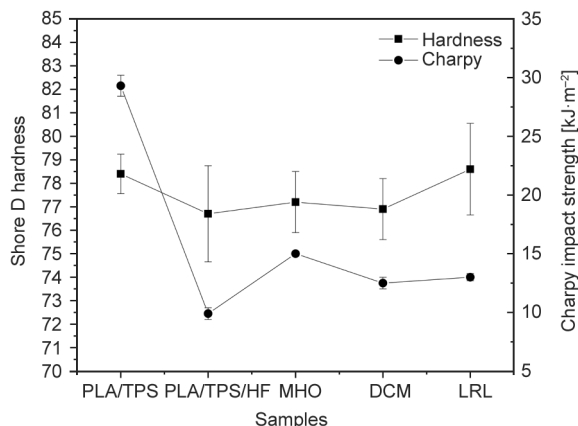


Figure 3. Shore D hardness and impact energy absorption of PLA/TPS sample and PLA/TPS/HF samples without compatibilizer and compatibilized.

where an impact absorption energy of $15 \text{ kJ}\cdot\text{m}^{-2}$ is obtained, representing an increase of 51.5% concerning the sample without compatibilization. This increase in energy absorption may be due to two reasons, one of them being the plasticizing effect caused by the MHO. It has been shown that maleinized vegetable oils act as a plasticizer in polymers, leading to an increase in the mobility of the polymer chains caused by an increase in the free volume and a reduction in the secondary interactions between them. On the other hand, the maleic anhydride groups of MHO can react with the hydroxyl groups of PLA, TPS, and HF, improving the compatibility between them and thus reducing their brittleness [37]. A similar effect can be observed in the DCM and LRL compatibilized samples, where energy absorption values of 12.5 and $13 \text{ kJ}\cdot\text{m}^{-2}$, respectively, are achieved.

Regarding the Shore D hardness, the unreinforced PLA/TPS sample shows a value of 78.4 Shore D. As can be seen, the hardness of the blend is hardly affected after the incorporation of HF and the different compatibilizers, obtaining values very similar to those of the unreinforced sample.

3.2. Thermal properties of PLA/TPS samples

The thermal properties of the PLA/TPS blend and the PLA/TPS/HF composites without compatibilization and compatibilized PLA/TPS/HF composites have been studied by DSC and TGA. Figure 4 shows the DSC thermograms of the different samples, while Table 2 shows the main thermal parameters obtained from the curves. All tests on each sample have been carried out 3 times. As can be seen, the PLA/TPS blend presents a glass transition temperature (T_g) of 62.2°C , a cold crystallization temperature (T_{cc}) of 95.8°C , and a melting temperature (T_m) of 168.9°C . These values are very similar to those obtained by Ferri *et al.* [35] for the PLA/TPS samples. Incorporating the HF reinforcement in the blend results in a slight reduction of the T_g , T_{cc} , and T_m , obtaining values of 60.5 , 89.6 , and 166.7°C , respectively. In addition, a decrease in the crystallinity of the blend is also observed after incorporating the filler, from 32.6% for the unreinforced blend to 24.6% for the reinforced blend. These results show how the HF reinforcement hinders the folding process of the polymer chains, thus preventing the formation of crystals

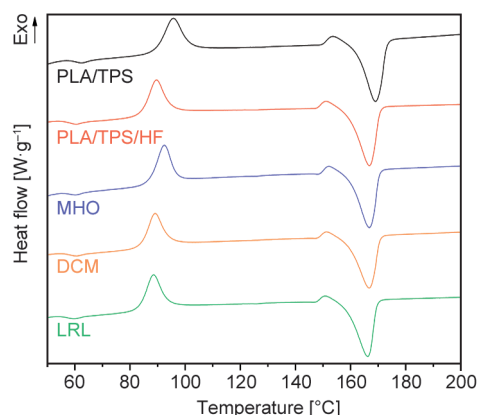


Figure 4. Calorimetric curves of PLA/TPS sample and PLA/TPS/HF samples without compatibilizer and compatibilized PLA/TPS/HF samples.

Table 2. Thermal properties of PLA/TPS sample and PLA/TPS/HF samples without compatibilizer and compatibilized PLA/TPS/HF samples obtained by differential scanning calorimetry.

Sample	T_g [°C]	T_{cc} [°C]	ΔH_{cc} [J·g ⁻¹]	T_m [°C]	ΔH_m [J·g ⁻¹]	X_c [%]
PLA/TPS	62.2±0.7	95.8±1.1	17.3±0.5	168.9±3.4	41.6±1.5	32.6±0.5
PLA/TPS/HF	60.5±0.5	89.6±0.9	14.2±0.1	166.7±2.1	32.5±1.1	24.6±0.6
MHO	60.7±0.6	92.6±0.7	13.8±0.2	166.7±2.9	35.2±0.9	28.7±0.6
DCM	60.7±0.2	89.1±1.2	12.9±0.4	166.5±3.2	36.9±1.8	32.2±0.8
LRL	60.0±0.3	88.6±0.4	14.1±0.4	166.1±1.7	31.9±1.7	23.9±0.5

[38]. Incorporating the different compatibilizers in the reinforced blend hardly affects its T_g and T_m . However, it is observed that the incorporation of MHO leads to a slight increase in the T_{cc} , from 89.6 °C for the composite without compatibilization to 92.6 °C for the composite compatibilized with MHO. This increase in T_{cc} in the MHO compatibilized sample may be related to the increase in compatibilization between the different constituents, which hinders the crystallization of the polymer chains. Moreover, it can be observed that the incorporation of MHO in the PLA/TPS/HF composite gives rise to a slight increase in crystallinity, obtaining values of 28.7%, representing an increase of 4.1% concerning the composite without compatibilization. This is due to the plasticizing effect of the modified oil that favors the mobility of the chains, leading to the formation of crystals [39].

The thermal stability of the different formulations obtained was studied by thermogravimetry. Figure 5 shows the thermogravimetric curves and the first derivative of these curves (DTG) of the PLA/TPS blend and of the PLA/TPS/HF biocomposites without compatibilization and compatibilized. In addition, Table 3 shows the degradation onset temperature (T_0) values, the temperature at which the samples show a 5% mass loss, and the maximum degradation temperature obtained from the DTG curves of the different formulations, as in the DSC, all tests on each sample have been carried out 3 times. As can be seen, the PLA/TPS blend without reinforcement presents a degradation onset temperature of 301.3 °C and a maximum degradation temperature of 339.1 °C. Adding the HF reinforcement in the blend reduces the thermal stability of the blend, obtaining a T_0 of

Table 3. Thermal properties of PLA/TPS sample and PLA/TPS/HF samples without compatibilizer and compatibilized PLA/TPS/HF samples obtained by thermogravimetry.

Sample	T_0 [°C]	T_{max} [°C]
PLA/TPS	301.3±1.4	339.1±3.1
PLA/TPS/HF	269.3±2.4	324.5±2.2
MHO	263.5±3.1	325.5±1.8
DCM	275.1±2.1	321.1±2.3
LRL	276.4±2.3	322.8±1.9

269.3 °C and a T_{max} of 324.5 °C for this sample. This decrease in both temperatures is due to the lower thermal stability of the lignocellulosic reinforcement, the one which begins its decomposition around 283.7 °C, which contributes negatively to the thermal stability of the composite. As can be seen in Table 3, the incorporation of the different compatibilizers hardly affects the T_{max} of the composite. However, different behavior is observed at T_0 according to the type of compatibilizer used. In this case, it can be seen how the incorporation of MHO and LRL results in a slight reduction of the T_0 concerning the composite without compatibilization, obtaining values of 263.5 and 276.4 °C, respectively. On the other hand, adding DCM increases the degradation onset temperature up to 275.1 °C.

3.3. Melt index of PLA/TPS samples

The melt flow index (MFI) analysis is interesting from the point of view of material manufacturing, as it determines how the material flows in the molten state. In this case, the aim is to analyze the effect of the incorporation of the lignocellulosic filler and the different compatibilizers on the melt viscosity of the

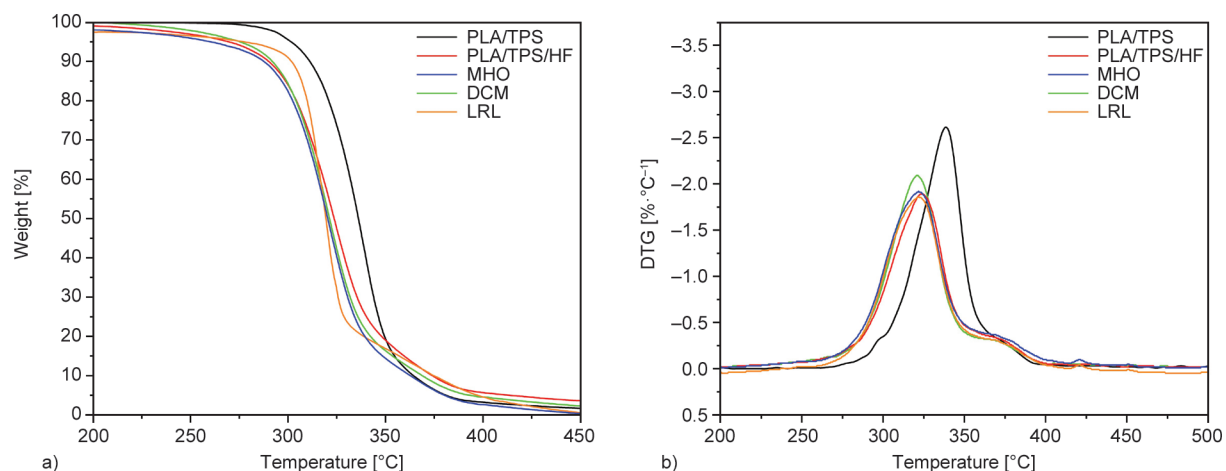


Figure 5. Thermogravimetric (TGA) curves (a) and its first derivative (DTG) (b) of the PLA/TPS sample and the PLA/TPS/HF samples without compatibilizer and compatibilized PLA/TPS/HF samples.

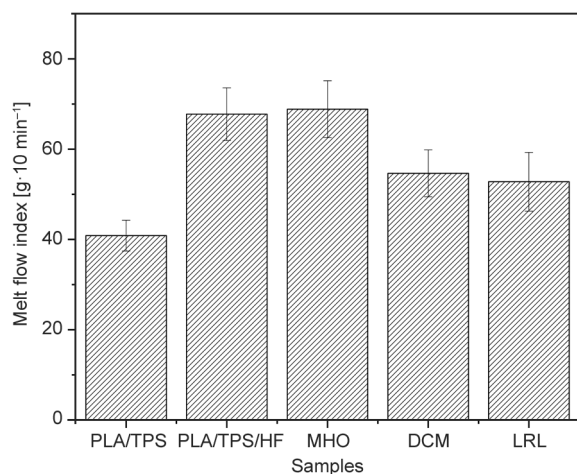


Figure 6. Melt Flow index of PLA/TPS sample and PLA/TPS/HF samples without compatibilizer and compatibilized PLA/TPS/HF samples.

PLA/TPS blend, taking into account that the relationship between MFI and viscosity is inverse and, therefore higher MFI values correspond to a lower melt viscosity [40]. Figure 6 shows the MFI of the PLA/TPS blend and the PLA/TPS/HF composites without compatibilization and compatibilized PLA/TPS/HF composites. As shown in Figure 6, the PLA/TPS blend has a melt flow index of $40 \text{ g} \cdot 10 \text{ min}^{-1}$, and after incorporating the filler, the melt flow index increases to around $67 \text{ g} \cdot 10 \text{ min}^{-1}$, an increase of about 65%. Therefore, the HF load's presence reduced the material's viscosity. This increase in the flow rate may be due to the oil contained in the lignocellulosic residue. Hemp seed has a high oil content, between 28 and 35% [41], which can act as a lubricant during the processing of the material, thus reducing the viscosity of the material [42]. On the other hand, the incorporation of MHO in the PLA/TPS/HF sample results in a slight increase in the melt flow index due to better compatibility of the different constituents of the composite [43]. Finally, it can be observed that the blend is compatible with DCM and LRL. However, it presents higher flow index values than the blend without reinforcement. These are lower than those of the composite without compatibilization, obtaining, in this case, flow index values of 54.6 and $52.7 \text{ g} \cdot 10 \text{ min}^{-1}$ for the composite compatibilized with DCM and LRL, respectively.

3.4. Morphological properties of PLA/TPS samples

Figure 7 shows the FESEM images of the fracture surface of the PLA/TPS blend and the PLA/TPS

samples reinforced with HF, both non-compatibilized and compatibilized. As can be seen, the fracture surface of the PLA/TPS sample (Figure 7a) shows a low roughness, which indicates the sample's brittleness. Furthermore, phase separation between both polymers can be observed, which can be seen by small spheres embedded in the PLA matrix [36]. This phase separation is mainly due to the difference in polarity between the two materials since PLA is a highly hydrophobic polymer. At the same time, TPS is hydrophilic – this lack of miscibility results in a brittle material. After the incorporation of the lignocellulosic filler into the PLA/TPS blend, an increase in the roughness of the fracture surface can be observed (Figure 7b). In addition, no agglomerates can be distinguished in the matrix, which indicates good load dispersion. In this sample, small voids can be observed on the fracture surface, corresponding to the HF particles released during the impact test due to the lack of interaction between them and the polymer matrix. The lack of continuity of the matrix due to the presence of the particles leads to embrittlement of the material, as observed in the mechanical properties. The addition of petrochemical compatibilizers such as DCM (Figure 7d) and LRL (Figure 7e) hardly modifies the fracture surface of the material, but the addition of MHO results in a more homogeneous surface, without the presence of phase separation, due to the compatible effect of the modified oil. This improvement in compatibility due to the presence of MHO, together with the plasticizing effect of MHO, results in a slight increase in the ductile mechanical properties of the sample, as observed above.

3.5. Disintegration in controlled compost soil of PLA/TPS samples

Figure 8 depicts the weight loss during the disintegration process of the PLA/TPS blend and the non-compatibilized and compatibilized PLA/TPS/HF composites. On the other hand, Figure 9 illustrates the visual appearance of the different samples during the conducted disintegration process. As observed, the PLA/TPS blend exhibits a 9 day incubation period during which the sample undergoes minimal disintegration, with a weight loss of less than 1%. After this period, the sample begins to disintegrate rapidly, with a weight loss exceeding 90% after 21 days. Figure 8 shows that the PLA/TPS blend becomes whiter at the 7 day mark. This phenomenon

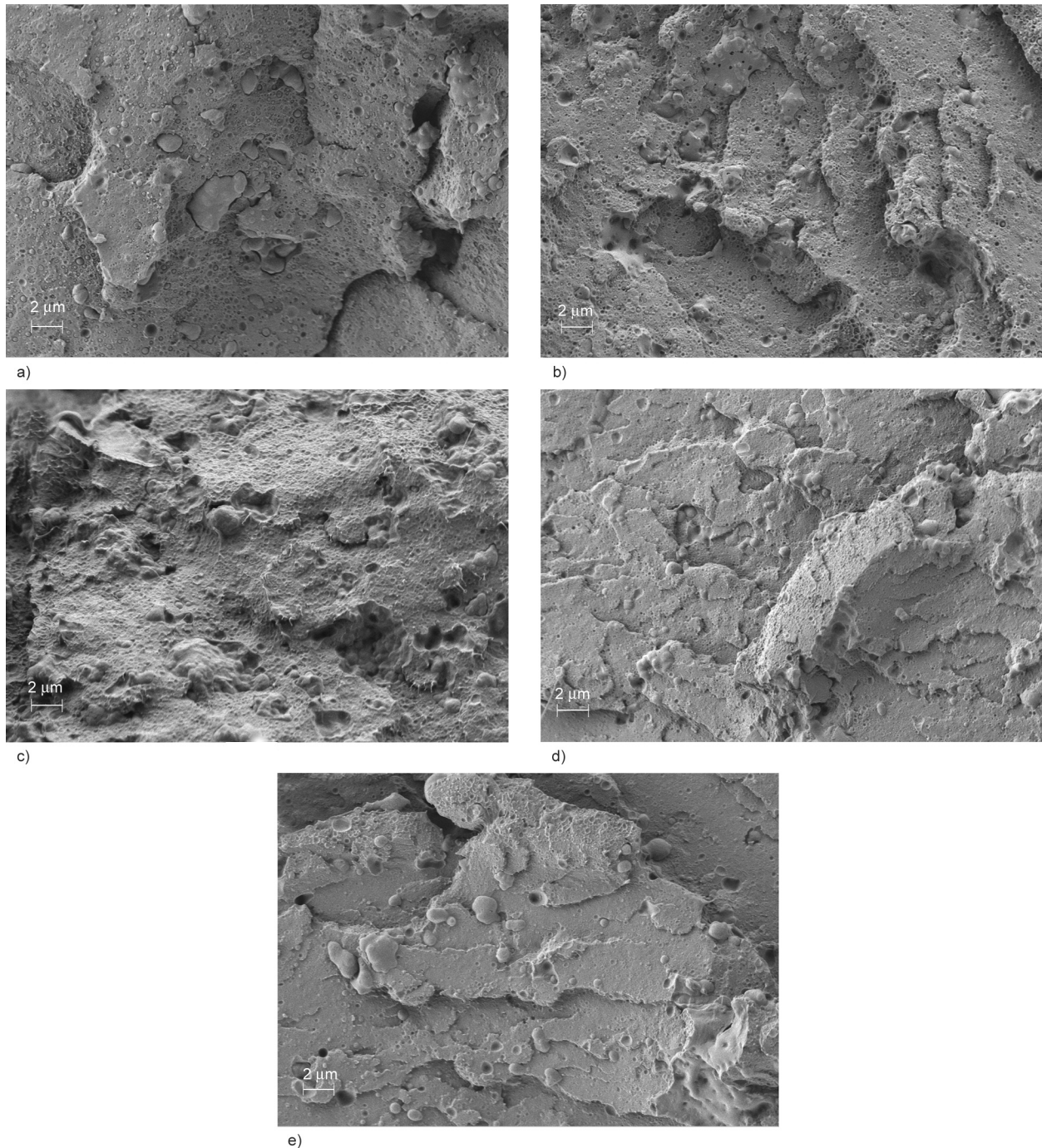


Figure 7. FESEM images at 2000× of the fracture surface of a) PLA/TPS; b) PLA/TPS/HF; c) MHO; d) DCM; e) LRL.

is also observed in the HF-reinforced samples. It is attributed to an increase in the crystallinity of PLA, as its T_g is close to the test temperature (58 °C). This increase in chain mobility and alignment leads to an enhancement in the material's opacity. On the other hand, adding HF filler to the PLA/TPS blend eliminates its incubation period, resulting in rapid degradation within the first 7 days, with a mass loss approaching 18%. Furthermore, at this point, the sample becomes brittle and loses its structural integrity. The disappearance of the incubation period

in the PLA/TPS/HF sample is attributed to the highly hydrophilic lignocellulosic filler, which facilitates the transfer of water, enzymes, and microorganisms into the matrix. This accelerates its disintegration during the initial days [39]. However, regarding the total disintegration time, it can be observed that the incorporation of HF results in an extended degradation time compared to the unreinforced blend, reaching 90% mass loss at 35 days. This is attributed to the slower disintegration rate of the lignocellulosic filler compared to PLA and TPS [44]. Finally, in Figure 8, it

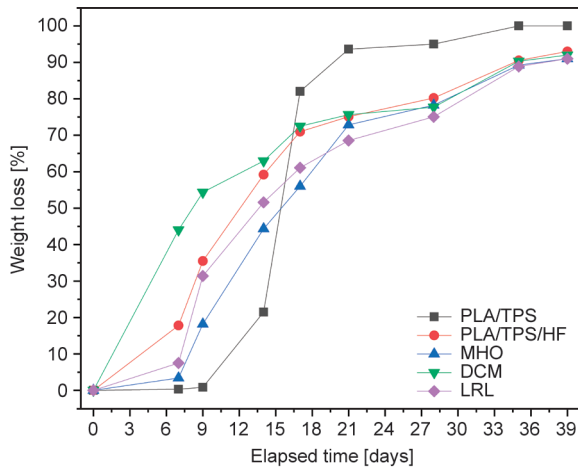


Figure 8. Weight loss concerning time during the disintegration test in controlled compost soil of PLA/TPS samples and of PLA/TPS/HF samples without compatibilizer and compatibilized PLA/TPS/HF samples.

can be observed that incorporating different compatibilizers has little effect on the total degradation time of the composite, with a 90% degradation rate achieved at 35 days for all compatibilized samples. However, the compatibilizers do influence the incubation period of the sample. In this case, adding MHO and LRL increases the incubation period of the composite compared to the non-compatibilized sample, resulting in degradation rates of 3.4 and 7.5% at 7 days for the MHO and LRL compatibilized samples,

respectively. Nevertheless, as shown in Figure 9, the MHO-compatibilized sample maintains its integrity at this time, while the LRL-compatibilized sample is completely fractured. This highlights the effectiveness of MHO as a compatibilizer, as its incorporation enhances the interaction between the different constituents, making it more challenging for them to disintegrate during the initial days of testing. Furthermore, it can be observed that the disintegration rate of the sample compatibilized with MHO is lower than that of the reinforced sample without compatibilization throughout the test.

3.6. Color properties of PLA/TPS samples

The visual appearance of the PLA/TPS sample and the PLA/TPS/HF composites with and without compatibilizer can be observed in Figure 10. Furthermore, Table 4 presents the CIELab color space coordinates values for each formulation and the color difference compared to the unmodified PLA/TPS blend. As observed, the unreinforced PLA/TPS blend exhibits a whitish color, with L^* , a^* , and b^* coordinates of 84.7, 0.045, and 6.2, respectively. As Figure 10 shows, adding HF filler to the blend imparts a brown hue to the material, giving it a wood-like appearance. This is attributed to the intrinsic color of the lignocellulosic reinforcement. Table 4 shows that incorporating the reinforcement reduces

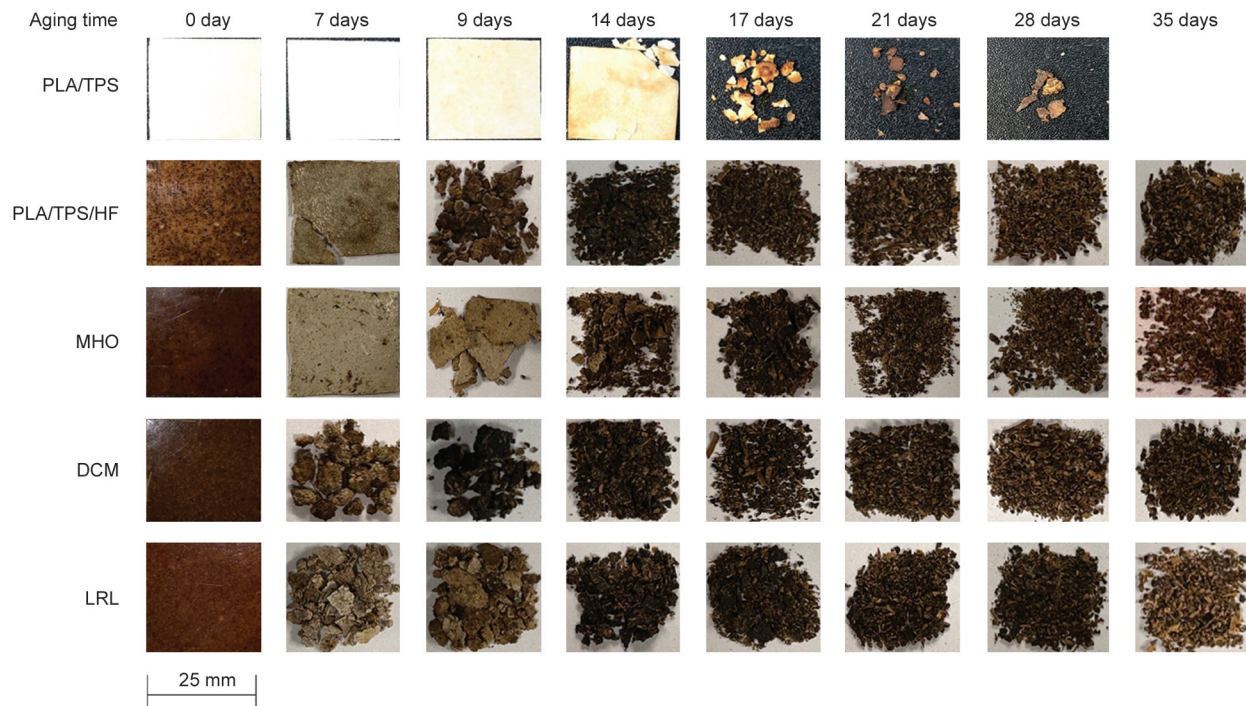


Figure 9. The visual aspect of the disintegration test on controlled compost soil of PLA/TPS samples and PLA/TPS/HF samples without compatibilizer and compatibilized PLA/TPS/HF samples.



Figure 10. The visual appearance of PLA/TPS samples and PLA/TPS/HF samples without compatibilizer and compatibilized PLA/TPS/HF samples.

the luminosity (L^*) values and shifts the b^* values towards higher values, indicating a yellowing of the samples. A similar behavior was observed by Yoksan *et al.* [45] when incorporating different amounts of water lentil flour into PLA/TPS blends. On the other hand, it can also be observed that reinforced samples exhibit small dark spots on the material's surface. This is attributed to the formation of aggregates of the reinforcement during processing due to its highly hydrophilic nature. The presence of such aggregates is more pronounced in the non-compatibilized sample, thus the addition of compatibilizers enhances the dispersion of the reinforcement in the polymer matrix, resulting in a more uniform surface color. Comparing the compatibilized composites, it can be seen in Table 4 that the L^* , a^* , and b^* values among them are very similar, indicating that the incorporation of compatibilizers has minimal impact on the color of the samples. However, it is noticeable that the sample compatibilized with MHO exhibits a darker brown hue than the others, as evidenced by a lower

Table 4. CIELAB coordinates and total color difference (ΔE) of PLA/TPS sample and PLA/TPS/HF samples without compatibilizer and compatibilized.

Sample	L^*	a^*	b^*	ΔL
PLA/TPS	84.7±0.01	0.04±0.03	6.2±0.02	–
PLA/TPS/HF	48.7±0.02	3.31±0.02	10.1±0.08	–36.0±0.01
MHO	40.5±0.01	5.03±0.06	14.7±0.05	–44.2±0.01
DCM	44.9±0.01	4.21±0.05	11.7±0.07	–39.8±0.01
LRL	43.7±0.01	6.25±0.05	11.8±0.05	–41.0±0.01

L^* value and a slight increase in the b^* coordinate. This darker tone in the MHO-compatibilized sample is attributed to the orange-red color hemp oil acquires after the maleinization process [46].

4. Conclusions

In conclusion, the investigation into the PLA/TPS blend and its composites containing HF reinforcement, both with and without various compatibility agents, has yielded valuable insights into their mechanical, thermal, degradation, and visual characteristics. The inclusion of HF had a notable impact on reducing the tensile mechanical properties of the PLA/TPS blend, leading to decreased tensile strength, Young's modulus, and elongation at break. This decline can be attributed to stress concentration phenomena and the limited interaction between HF residue and the polymer matrix. However, the incorporation of different compatibility agents had a limited effect on the tensile properties of the non-compatibilized sample (PLA/TPS/HF), with similar values for Young's modulus, tensile strength, and elongation at break. Maleinized hemp oil (MHO) was an exception, which increased elongation at the break by 27.3%, owing to enhanced compatibility between PLA, TPS, and HF and MHO's plasticizing effect. Similar effects were observed in the DCM and LRL compatibilized samples, though the increase in energy absorption was less pronounced.

Regarding thermal properties, the addition of HF resulted in a minor reduction in the glass transition temperature (T_g), cold crystallization temperature (T_{cc}), and melting temperature (T_m) of the blend. This decrease in crystallinity was due to HF reinforcement hindering polymer chain folding. Thermal stability was assessed via thermogravimetry, revealing that HF reinforcement decreased the composite's degradation onset temperature (T_0) and maximum degradation temperature (T_{max}). The choice of compatibility agent had variable effects on T_0 , with MHO and LRL reducing it while DCM increased it.

The melt flow index (MFI) analysis indicated that adding HF reduced melt viscosity, likely because of HF's oil content acting as a lubricant. Compatibility agents had minimal impact on MFI, but, in general, they increased flow indices. Examination of the fracture surface revealed that HF reinforcement heightened roughness, resulting in phase separation between PLA and TPS, indicating brittleness. However, MHO compatibility improved homogeneity

and reduced phase separation, enhancing ductility. Degradation behavior demonstrated that HF incorporation eliminated the incubation period and accelerated degradation due to HF's highly hydrophilic nature. Compatibility agents influenced the incubation period, with MHO significantly delaying degradation. The addition of HF introduced a brown hue and yellowing to the material due to HF's intrinsic color. Compatibility agents improved reinforcement dispersion and surface uniformity, with MHO-compatible samples exhibiting a darker brown shade attributed to the color of hemp oil following the maleinization process.

To summarize, this investigation underscores the intricate relationship between HF reinforcement, compatibility agents, and the properties of PLA/TPS composites. Compatibility, especially when using MHO, plays a pivotal role in enhancing harmonious blending, elevating specific material properties, and prolonging degradation, thereby presenting a promising avenue for the development of sustainable biocomposites.

Acknowledgements

This research work was funded by the Ministry of Science and Innovation through – ‘Retos de la Sociedad’, project reference PID2020-119142RA-I00 and is part of the grant PID2020-116496RB-C22, funded by MCIN/AEI/10.13039/501100011033 and the grant TED2021-131762A-I00, funded by MCIN/AEI/10.13039/501100011033 and by the European Union ‘NextGenerationEU’/PRTR. The authors also thank Generalitat Valenciana-GVA for funding this research through the grant numbers AICO/2021/025 and CIGE/2021/094. Funded with Aid for First Research Projects (PAID-06-22), Vice-rectorate for Research of the Universitat Politècnica de València (UPV). J. Gomez-Caturla wants to thank FPU20/01732 grant funded by MCIN/AEI/10.13039/501100011033 and by ESF Investing in your future.

References

- [1] Auras R., Harte B., Selke S.: An overview of polylactides as packaging materials. *Macromolecular Bioscience*, **4**, 835–864 (2004).
<https://doi.org/10.1002/mabi.200400043>
- [2] Bhardwaj R., Mohanty A. K.: Advances in the properties of polylactides based materials: A review. *Journal of Biobased Materials and Bioenergy*, **1**, 191–209 (2007).
<https://doi.org/10.1166/jbmb.2007.023>
- [3] Slomkowski S., Penczek S., Duda A.: Polylactides-An overview. *Polymers for Advanced Technologies*, **25**, 436–447 (2014).
<https://doi.org/10.1002/pat.3281>
- [4] Cheng H-Y., Yang Y-J., Li S-C., Hong J-Y., Jang G-W.: Modification and extrusion coating of polylactic acid films. *Journal of Applied Polymer Science*, **132**, 42472 (2015).
<https://doi.org/10.1002/app.42472>
- [5] Ingraio C., Tricase C., Cholewa-Wójcik A., Kawecka A., Rana R., Siracusa V.: Polylactic acid trays for fresh-food packaging: A carbon footprint assessment. *Science of the Total Environment*, **537**, 385–398 (2015).
<https://doi.org/10.1016/j.scitotenv.2015.08.023>
- [6] Anderson K. S., Schreck K. M., Hillmyer M. A.: Toughening polylactide. *Polymer Reviews*, **48**, 85–108 (2008).
<https://doi.org/10.1080/15583720701834216>
- [7] Hwang S. W., Shim J. K., Selke S., Soto-Valdez H., Rubino M., Auras R.: Effect of maleic-anhydride grafting on the physical and mechanical properties of poly(L-lactic acid)/starch blends. *Macromolecular Materials and Engineering*, **298**, 624–633 (2013).
<https://doi.org/10.1002/mame.201200111>
- [8] Wang Y. B., Hillmyer M. A.: Polyethylene-poly(L-lactide) diblock copolymers: Synthesis and compatibilization of poly(L-lactide)/polyethylene blends. *Journal of Polymer Science Part A: Polymer Chemistry*, **39**, 2755–2766 (2001).
<https://doi.org/10.1002/pola.1254>
- [9] Reddy N., Nama D., Yang Y. Q.: Polylactic acid/polypropylene polyblend fibers for better resistance to degradation. *Polymer Degradation and Stability*, **93**, 233–241 (2008).
<https://doi.org/10.1016/j.polymdegradstab.2007.09.005>
- [10] Garcia-Masabet V., Perez O. S., Cailloux J., Abt T., Sanchez-Soto M., Carrasco F., MasPOCH M. L.: PLA/PA bio-blends: Induced morphology by extrusion. *Polymers*, **12**, 10 (2020).
<https://doi.org/10.3390/polym12010010>
- [11] Kaseem M., Ko Y. G.: Melt flow behavior and processability of polylactic acid/polystyrene (PLA/PS) polymer blends. *Journal of Polymers and the Environment*, **25**, 994–998 (2017).
<https://doi.org/10.1007/s10924-016-0873-5>
- [12] Iannace S., Ambrosio L., Huang S. J., Nicolais L.: Poly(3-hydroxybutyrate)-*co*-(3-hydroxyvalerate)/poly-L-lactide blends: Thermal and mechanical properties. *Journal of Applied Polymer Science*, **54**, 1525–1535 (1994).
<https://doi.org/10.1002/app.1994.070541017>
- [13] Takagi Y., Yasuda R., Yamaoka M., Yamane T.: Morphologies and mechanical properties of polylactide blends with medium chain length poly(3-hydroxyalkanoate) and chemically modified poly(3-hydroxyalkanoate). *Journal of Applied Polymer Science*, **93**, 2369–2369 (2004).
<https://doi.org/10.1002/app.20734>
- [14] Fortelny I., Ujcic A., Fambri L., Slouf M.: Phase structure, compatibility, and toughness of PLA/PCL blends: A review. *Frontiers in Materials*, **6**, 206 (2019).
<https://doi.org/10.3389/fmats.2019.00206>

- [15] Hu X., Su T., Li P., Wang Z.: Blending modification of PBS/PLA and its enzymatic degradation. *Polymer Bulletin*, **75**, 533–546 (2018).
<https://doi.org/10.1007/s00289-017-2054-7>
- [16] Noorizzah I., Ab Wahab M. K., Uy Lan D. N.: Mechanical and physical properties of polylactic acid (PLA)/thermoplastic starch (TPS) blends. *Journal of Polymer Materials*, **33**, 201–212 (2016).
- [17] Ke T., Sun X.: Effects of moisture content and heat treatment on the physical properties of starch and poly(lactic acid) blends. *Journal of Applied Polymer Science*, **81**, 3069–3082 (2001).
<https://doi.org/10.1002/app.1758>
- [18] Ilyas R. A., Sapuan S. M., Ibrahim R., Abral H., Ishak M. R., Zainudin E. S., Atilzah M. S. N., Nurazzi N. M., Atiqah A., Ansari M. N. M., Syafri E., Asrofi M., Sari N. H., Jumaidin R.: Effect of sugar palm nanofibrillated cellulose concentrations on morphological, mechanical and physical properties of biodegradable films based on agro-waste sugar palm (*Arenga pinnata* (Wurmb.) Merr) starch. *Journal of Materials Research and Technology-Jmr&T*, **8**, 4819–4830 (2019).
<https://doi.org/10.1016/j.jmrt.2019.08.028>
- [19] Baker W. E., Scott C., Hu G. H.: Reactive polymer blending. Hanser, München (2001).
- [20] Hwang S. W., Shim J. K., Selke S., Soto-Valdez H., Rubino M., Auras R.: Effect of maleic anhydride on the reactive blending of poly(L-lactic acid)/starch. in '18th IAPRI World Packaging Conference, San Luis Obispo, USA' 508–515 (2012).
- [21] Jariyasakoolroj P., Chirachanchai S.: Silane modified starch for compatible reactive blend with poly(lactic acid). *Carbohydrate Polymers*, **106**, 255–263 (2014).
<https://doi.org/10.1016/j.carbpol.2014.02.018>
- [22] Ibrahim N., Ab Wahab M. K., Uylan D. N., Ismail H.: Physical and degradation properties of polylactic acid and thermoplastic starch blends – Effect of citric acid treatment on starch structures. *Bioresources*, **12**, 3076–3087 (2017).
<https://doi.org/10.15376/biores.12.2.3076-3087>
- [23] Acioli-Moura R., Sun X. S.: Thermal degradation and physical aging of poly(lactic acid) and its blends with starch. *Polymer Engineering and Science*, **48**, 829–836 (2008).
<https://doi.org/10.1002/pen.21019>
- [24] Xiong Z., Ma S., Fan L., Tang Z., Zhang R., Na H., Zhu J.: Surface hydrophobic modification of starch with bio-based epoxy resins to fabricate high-performance polylactide composite materials. *Composites Science and Technology*, **94**, 16–22 (2014).
<https://doi.org/10.1016/j.compscitech.2014.01.007>
- [25] Raquez J.-M., Narayan R., Dubois P.: Recent advances in reactive extrusion processing of biodegradable polymer-based compositions. *Macromolecular Materials and Engineering*, **293**, 447–470 (2008).
<https://doi.org/10.1002/mame.200700395>
- [26] Alikarami N., Abrisham M., Huang X., Panahi-Sarmad M., Zhang K., Dong K., Xiao X.: Compatibilization of PLA grafted maleic anhydride through blending of thermoplastic starch (TPS) and nanoclay nanocomposites for the reduction of gas permeability. *International Journal of Smart and Nano Materials*, **13**, 130–151 (2022).
<https://doi.org/10.1080/19475411.2022.2051639>
- [27] Jafari M., Jalalifar N., Kaffashi B.: Rheological properties and crystallization behavior of modified polylactic acid using lauroyl peroxide and glycidyl methacrylate. *Journal of Applied Polymer Science*, **138**, 49924 (2021).
<https://doi.org/10.1002/app.49924>
- [28] Nyambo C., Mohanty A. K., Misra M.: Effect of maleated compatibilizer on performance of PLA/wheat straw-based green composites. *Macromolecular Materials and Engineering*, **296**, 710–718 (2011).
<https://doi.org/10.1002/mame.201000403>
- [29] Chang K., Robertson M. L., Hillmyer M. A.: Phase inversion in polylactide/soybean oil blends compatibilized by poly(isoprene-*b*-lactide) block copolymers. *ACS Applied Materials and Interfaces*, **1**, 2390–2399 (2009).
<https://doi.org/10.1021/am900514v>
- [30] Ferri J. M., Garcia-Garcia D., Carbonell-Verdu A., Fenollar O., Balart R.: Poly(lactic acid) formulations with improved toughness by physical blending with thermoplastic starch. *Journal of Applied Polymer Science*, **135**, 45751 (2018).
<https://doi.org/10.1002/app.45751>
- [31] Lerma-Canto A., Gomez-Caturla J., Herrero-Herrero M., Garcia-Garcia D., Fombuena V.: Development of polylactic acid thermoplastic starch formulations using maleinized hemp oil as biobased plasticizer. *Polymers*, **13**, 1392 (2021).
<https://doi.org/10.3390/polym13091392>
- [32] Meng B., Deng J., Liu Q., Wu Z., Yang W.: Transparent and ductile poly(lactic acid)/poly(butyl acrylate) (PBA) blends: Structure and properties. *European Polymer Journal*, **48**, 127–135 (2012).
<https://doi.org/10.1016/j.eurpolymj.2011.10.009>
- [33] Ghari, H. S., Nazockdast, H.: Morphology development and mechanical properties of PLA/differently plasticized starch (TPS) binary blends in comparison with PLA/dynamically crosslinked 'TPS plus EVA' ternary blends. *Polymer*, **245**, 124729 (2022).
<https://doi.org/10.1016/j.polymer.2022.124729>
- [34] García-García D., Carbonell A., Samper M., García-Sanoguera D., Balart R.: Green composites based on polypropylene matrix and hydrophobized spend coffee ground (SCG) powder. *Composites Part B: engineering*, **78**, 256–265 (2015).
<https://doi.org/10.1016/j.compositesb.2015.03.080>

- [35] Ferri J., Garcia-Garcia D., Sánchez-Nacher L., Fenollar O., Balart R.: The effect of maleinized linseed oil (MLO) on mechanical performance of poly(lactic acid)-thermoplastic starch (PLA-TPS) blends. *Carbohydrate polymers*, **147**, 60–68 (2016).
<https://doi.org/10.1016/j.carbpol.2016.03.082>
- [36] Akrami M., Ghasemi I., Azizi H., Karrabi M., Seyedabadi M.: A new approach in compatibilization of the poly(lactic acid)/thermoplastic starch (PLA/TPS) blends. *Carbohydrate Polymers*, **144**, 254–262 (2016).
<https://doi.org/10.1016/j.carbpol.2016.02.035>
- [37] Liminana P., Garcia-Sanoguera D., Quiles-Carrillo L., Balart R., Montanes N.: Optimization of maleinized linseed oil loading as a biobased compatibilizer in poly(butylene succinate) composites with almond shell flour. *Materials*, **12**, 685 (2019).
<https://doi.org/10.3390/ma12050685>
- [38] Quiles-Carrillo L., Montanes N., Sammon C., Balart R., Torres-Giner S.: Compatibilization of highly sustainable polylactide/almond shell flour composites by reactive extrusion with maleinized linseed oil. *Industrial Crops and Products*, **111**, 878–888 (2018).
<https://doi.org/10.1016/j.indcrop.2017.10.062>
- [39] Dominguez-Candela I., Gomez-Caturla J., Cardona S., Lora-Garcia J., Fombuena V. J. E. P. J.: Novel compatibilizers and plasticizers developed from epoxidized and maleinized chia oil in composites based on PLA and chia seed flour. *European Polymer Journal*, **173**, 111289 (2022).
<https://doi.org/10.1016/j.eurpolymj.2022.111289>
- [40] Junaedi H., Baig M., Dawood A., Albahkali E., Almajid A.: Effect of the matrix melt flow index and fillers on mechanical properties of polypropylene-based composites. *Materials*, **15**, 7568 (2022).
<https://doi.org/10.3390/ma15217568>
- [41] Kostić M. D., Joković N. M., Stamenković O. S., Rajković K. M., Milić P. S., Veljković V. B.: Optimization of hempseed oil extraction by n-hexane. *Industrial Crops and Products*, **48**, 133–143 (2013).
<https://doi.org/10.1016/j.indcrop.2013.04.028>
- [42] Suaduang N., Ross S., Ross G., Pratumshat S., Mahasaranon S.: Effect of spent coffee grounds filler on the physical and mechanical properties of poly(lactic acid) bio-composite films. *Materials Today: Proceedings*, **17**, 2104–2110 (2019).
<https://doi.org/10.1016/j.matpr.2019.06.260>
- [43] Nasir M. H. M., Taha M. M., Razali N., Ilyas R. A., Knight V. F., Norrrahim M.: Effect of chemical treatment of sugar palm fibre on rheological and thermal properties of the PLA composites filament for FDM 3D printing. *Materials*, **15**, 8082 (2022).
<https://doi.org/10.3390/ma15228082>
- [44] Zandi A., Zanganeh A., Hemmati F., Mohammadi-Roshandeh J.: Thermal and biodegradation properties of poly(lactic acid)/rice straw composites: Effects of modified pulping products. *Irinian Polymer Journal*, **28**, 403–415 (2019).
<https://doi.org/10.1007/s13726-019-00709-3>
- [45] Yoksan R., Boontanimitr A., Klompong N., Phothongsurakun T.: Poly(lactic acid)/thermoplastic cassava starch blends filled with duckweed biomass. *Journal of Biological Macromolecules*, **203**, 369–378 (2022).
<https://doi.org/10.1016/j.ijbiomac.2022.01.159>
- [46] Perez-Nakai A., Lerma-Canto A., Dominguez-Candela I., Garcia-Garcia D., Ferri J. M., Fombuena V.: Comparative study of the properties of plasticized polylactic acid with maleinized hemp seed oil and a novel maleinized brazil nut seed oil. *Polymers*, **13**, 2376 (2021).
<https://doi.org/10.3390/polym13142376>